IEEE Access
Multidisciplinary ⋮ Rapid Review ⋮ Open Access Journal

Received February 5, 2020, accepted February 18, 2020, date of publication February 27, 2020, date of current version March 19, 2020.

Digital Object Identifier 10.1109/ACCESS.2020.2976841

Wearable Carbon Monoxide Sensors Based on Hybrid Graphene/ZnO Nanocomposites

LISTYA UTARI[1], NI LUH WULAN SEPTIANI[1], SUYATMAN[1], NUGRAHA[1,2], LEVY OLIVIA NUR[3], HUTOMO SURYO WASISTO[4,5], AND BRIAN YULIARTO[1,2]

[1]Advanced Functional Materials Laboratory, Department of Engineering Physics, Faculty of Industrial Technology, Institut Teknologi Bandung, Bandung 40132, Indonesia
[2]Research Center for Nanoscience and Nanotechnology, Institut Teknologi Bandung, Bandung 40132, Indonesia
[3]School of Electrical Engineering, Telkom University, Bandung 40257, Indonesia
[4]Institute of Semiconductor Technology (IHT), Technische Universität Braunschweig, 38106 Braunschweig, Germany
[5]Laboratory for Emerging Nanometrology (LENA), Technische Universität Braunschweig, 38106 Braunschweig, Germany

Corresponding author: Brian Yuliarto (brian@tf.itb.ac.id)

This work was supported in part by the Ministry of Education and Culture and the Institut Teknologi Bandung (ITB). The work of Hutomo Suryo Wasisto was supported in part by the Lower Saxony Ministry for Science and Culture (N-MWK) for the LENA-OptoSense, and in part by the Indonesian-German Center for Nano and Quantum Technologies (IG-Nano) and RISTEKDIKTI. The work of Brian Yuliarto was supported by the World Class University (WCU) Program through the Ministry of Education and Culture, managed by the ITB.

ABSTRACT In this work, wearable resistive gas sensors based on hybrid graphene/zinc oxide (ZnO) nanocomposites were fabricated on a flexible cotton fabric and employed to monitor odorless and colorless carbon monoxide (CO). Dip-coating and chemical bath deposition (CBD) was used to deposit the graphene layer and grow the ZnO nanorods, respectively. The films were characterized by scanning electron microscopy (SEM), energy-dispersive X-ray spectroscopy (EDS), and X-Ray diffraction (XRD) to investigate their morphological structures, elemental composition, and crystal phase, respectively. Those characterizations were also confirming the growth of ZnO nanorods on the already-deposited graphene layer on fabrics. From the gas sensor measurements at room temperature, it was revealed that these graphene/ZnO nanocomposites were highly sensitive and selective towards CO gas at low concentration down to 10 ppm. The shortest response and recovery times of the sensors were measured to be 280 s and 45 s, respectively. Moreover, in comparison to bare graphene sensors, the surface modification by ZnO nanorods could obviously enhance the sensing response by up to 40% (i.e., doubled sensitivity). These flexible hybrid sensors are therefore expected to be a promising alternative for the existing rigid CO sensors in the market by offering unique nanostructures, low-cost fabrication, high flexibility, and good sensing performances.

INDEX TERMS Wearable gas sensor, carbon monoxide, graphene, zinc oxide, fabric-based sensor.

I. INTRODUCTION

Nowadays, air pollution has been considered as one of the major concerns in modern societies because it causes highly widespread damage to the environment and adverse health effect to humans. Various sources of air pollutants can be found in both indoor (e.g., homes and workplaces) and outdoor environments (e.g., industrial boilers, on-road and off-road vehicles, power plants, and petrochemical plants) [1], [2]. Besides particulate matters (PM) with various particle sizes, several toxic gases (e.g., nitrogen oxides (NO_x), sulfur dioxide (SO_2), and carbon monoxide (CO)) can highly decrease air quality. Thus, several attempts have been made to assess air quality for preventing the public from exposure to harmful gases and particles. The attempts were performed by continuously monitoring different types of airborne pollutants using portable sensor devices and subsequently providing a fast alert when their concentrations have reached levels beyond safety limits [3]–[8].

Among other toxic air pollutants, the detection of CO remains challenging due to its odorless and colorless characteristics. This gas has normally been produced by incomplete burning of fossil fuels, vehicle emissions, and industrial combustions [9], [10]. The health effects caused by CO on humans are depending on the CO concentration and the exposure time. Moreover, the World Health Organization (WHO)

The associate editor coordinating the review of this manuscript and approving it for publication was Praveen Gunturi.

sets the time-weighted average (TWA) exposure limit to CO of 9 ppm for 8 h [10], [11]. Typically, moderate exposure to CO leads to breathing difficulties, headache, nausea, dizziness, and tiredness. However, more fatal symptoms are induced when a person is exposed to a higher concentration of CO, e.g., vomiting, poor mental alertness, reduced muscular coordination, loss of consciousness, and even death [12]–[16].

As smart technology trends have now gradually changed human living, more and smarter devices have been developed and integrated into a system for specific tasks, e.g., air quality monitoring. In this case, stationary sensing devices have become less attractive, as they are bulky and heavy. Thus, sensors with higher flexibility and portability have been highly demanded by the societies to overcome that issue. To date, various wearable flexible sensors have been engineered for detecting different gases, i.e., CO, NO_2, hydrogen (H_2), ammonia (NH_3), carbon dioxide (CO_2), hydrogen sulfide (H_2S), and water vapor (humidity) [17]–[19]. They consist normally of the sensitive sensing nanomaterials that are transferred to or directly grown on different flexible substrates as sensor carriers (e.g., poly(methyl methacrylate) (PMMA) [20], poly(dimethylsiloxane) (PDMS) [21], polyimide (PI) [22], poly(ethylene naphthalate) (PEN) [23], poly(ethylene terephtha-late) (PET) [24], and cotton fabrics [25]). Among them, cotton fabrics are currently highly researched, not only because of their excellent properties (i.e., high flexibility, low cost, high moisture absorbency, good mechanical strength, good biocompatibility, and biodegradability), but also due to the fact that these substrates can be integrated as smart clothing to support the advancement of industrial revolution 4.0 [26], [27]. Currently, surface-modified cotton fabrics have been applied for several wearable devices, including UV filter [28]–[30], superhydrophobic functional garment [31], flame resistance composite [32], anti-bacterial component [33], and gas sensors [34]–[37].

In case of textile-based gas sensing devices, metal oxide (MOX) has been normally employed as a sensing material due to its good electrical, optical, optoelectronic, and gas-sensing properties [37]. Among various oxides, zinc oxide (ZnO) is considered as one of the most promising sensing materials owing to its low cost, high sensitivity, high chemical and thermal stabilities, biocompatibility, and high electron mobility [38], [39]. However, the gas-sensing performance of ZnO-based sensors is often limited by poor selectivity and high operating temperature, thereby leading to unsatisfactory performance and high-power consumption, respectively. To overcome those issues, other materials and architectures have been continuously researched, including graphene, which is a 2D allotrope of carbon with a honeycomb crystal lattice. Since its groundbreaking invention, which was awarded with the 2010 Nobel Prize in Physics, this one-atom-thick layer of graphite has been widely used in various electronic applications due to its excellent properties (i.e., good electronic conductivity, large specific area, and high carrier mobility at room temperature), rendering it highly attractive for room temperature gas sensors [38], [40], [41]. In fact, several graphene-based wearable sensors have been introduced for the detections of H_2, NH_3, H_2S, SO_2, CO_2, and NO_2 [42]. Moreover, further improvement has been made by combining those two prominent materials (i.e., MOX and graphene), which can then not only lower the optimum operating temperature, but also provide enhanced sensing response [43]–[48].

Herein, we report on the fabrication and characterization of wearable gas sensors based on graphene/ZnO composites grown on cotton fabrics via wet solution-based methods. The resulting graphene/ZnO nanostructure layers were characterized using energy-dispersive X-ray spectroscopy (EDS), X-Ray diffraction (XRD), and scanning electron microscopy (SEM) to investigate the elemental composition, crystallinity and morphological structures of graphene/ZnO layer, respectively. Meanwhile, the performance of the developed graphene/ZnO-based sensor was assessed in gas cross-sensitivity measurement series, demonstrating its potential for highly sensitive and selective gas sensors that can be integrated into daily living accessories (e.g., smart clothes).

II. EXPERIMENTAL

A. CHEMICAL SUBSTANCES

All chemicals used in the creation of hybrid G/ZnO nanostructures were analytical grade and commercially available products in the market. Zinc nitrate hexahydrate ($Zn(NO_3)_2.6H_2O$, 99%), triethylamine ($C_6H_{15}N$, 99.5%) from Fujifilm Wako Pure Chemical Corporation, Japan and hexamethylenetetramine (HMTA, $C_6H_{12}N_4$, $\geq$99.0%) from Tokyo Chemical Industry, Japan were used to grow ZnO seeds and nanorods, respectively. Graphene flakes (>99% carbon purity) from Skyspring Nanomaterials Inc., Houston, USA were employed as a basis material for graphene deposition on fabrics prior to ZnO decoration. Ethanol (C_2H_6O, 99.5%), isopropanol (C_3H_8O, 99.5%), and acetone (C_3H_6O, 99.5%) from Merck as well as distilled (DI) water were used to support the chemical reaction during the growths and cleaning processes of the samples.

B. HYBRID FLEXIBLE DEVICE FABRICATION

The cotton fabrics obtained from a typical laboratory coat, have specification that was listed on Table. S1. The fabric was cut into a size of 2 cm $\times$ 2 cm as seen in Fig. S1. These samples were cleaned in acetone, ethanol, isopropanol, and DI water by ultrasonication for 15 minutes. Afterward, they were dried at 70°C and subsequently fixed onto a glass microscope slide by Kapton®adhesive polyimide tape (Fig. 1).

The deposition of the graphene layer on the cotton fabrics was performed by the dry-dipping method. Graphene solution was firstly prepared by ultrasonication of graphene flakes in DI water for 30 minutes. The fabrics were dipped into the graphene solution under ultrasonication for 2 h

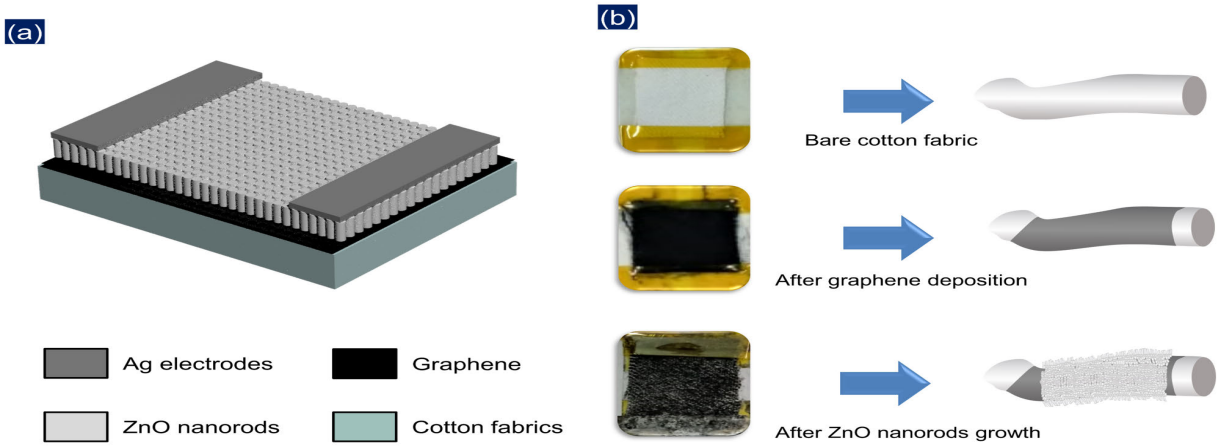

FIGURE 1. (a) Schematic diagram of the wearable CO sensor based on graphene/ZnO layers and (b) photographs of the original or non-coated fabric, graphene-coated fabric, and graphene/ZnO-coated fabric.

and then, dried at 70°C. To find a appropriate composition between graphene and ZnO, graphene concentration in the solution was varied to 0.0125 M (G1/Z2), 0.025 M (G1/Z1), and 0.05 M (G2/Z1) (Fig. 1(b)). Those four different samples were evaluated in terms of their sensing performances. In the next step, the graphene-coated fabrics were modified with ZnO seed layers deposited via a solution-based-method. The ZnO seed solution was prepared by dissolving 0.1 M $Zn(NO_3)_2.6H_2O$ in 2-propanol followed by subsequent heating at 75°C under magnetic stirring. After stirring for 15 minutes, 0.1 M triethylamine ($C_6H_{15}N$) was added into this solution as a sol stabilizer. The resulting mixture solution was stirred at 75°C for an additional 15 minutes before being cooled at room temperature. Once the seed solution had been prepared, the graphene-coated fabrics were directly dipped into it for 5 minutes and then rinsed with ethanol. These fabrics were dried at 80°C for 30 minutes.

The ZnO nanorod was grown on the ZnO seeded graphene-coated fabrics by chemical bath deposition (CBD) method. Prior to the CBD process, an aqueous solution containing 0.025 M $Zn(NO_3)_2.6H_2O$ and hexamethylenetetramine ($C_6H_{12}N_4$) (HMTA) was prepared as a zinc source. The HMTA was used to introduce steric hindrance effect and induce anisotropic growth of ZnO nanorod. The ZnO seeded graphene-coated fabrics were immersed in the solution and subsequently heated in an oven at 80 °C for 6 h. After the CBD process was finished, the fabrics were taken out and rinsed with DI water and then dried in air at room temperature (Fig. 1(b)).

C. CHARACTERIZATION METHODS

The morphologies and composition of samples were characterized by SEM (Hitachi, SU8000) integrated with Energy Dispersive Spectrometer (EDS). XRD of the deposited fabric was performed using a Rigaku SmartLab. Electrical resistance measurements of the developed samples were carried using a digital multimeter (Picotest M3500A (100Ω – 100MΩ)) in a 10 × 10 × 15 cm^3 sealed chamber. The samples were exposed by target gas for 15 minutes for investigating the response of the sensors. The compressed air was alternately introduced to the chamber to analyze the recovery time of the sensors. The sensing response (S) is calculated by measuring the percentage of resistance change upon exposure of the sensor to the gas, as described by the following equation:

$$\textit{Response}\,(\%) = \frac{R_a - R_g}{R_a} \times 100\% \qquad (1)$$

where Ra and Rg are the sensor resistances in ambient condition and upon exposure to the gas, respectively.

III. RESULTS AND DISCUSSION

A. MORPHOLOGICAL ANALYSIS

The flexible wearable CO sensor design is illustrated in Fig. 1(a), in which two silver (Ag) top electrodes are placed at both ends of the sensor connecting the graphene/ZnO nanorods on white cotton fabrics. The conditions of the sample during device processing are depicted in Fig. 1(b) where the color of fabrics was changing from white to black after its surfaces have been modified with graphene. Moreover, it was found that the composite G1/Z1 so strongly attached to the fabric that the composite was not detached after underwent sonication for 30 minutes in water (See Fig. S2).

To demonstrate its scalability and possibility for real use, the whole sensor component is made at a relatively large size (i.e., 2 × 2 cm^2). Graphene has flake shapes that are agglomerated due to their strong surface interaction (Fig. 2(a)). These nano-graphene platelets with various concentrations were successfully coated on the fabric surfaces chemical bath deposition (CBD) in an aqueous solution containing zinc nitrate ($Zn(NO_3)_2$) and HMTA (Fig. 2(b,c)). When zinc nitrate dissociates in the solution, the zinc ions (Zn^{2+}) react with water molecules to form the complex $(Zn(H_2O)_6)^{2+}$, which further decomposes into zinc

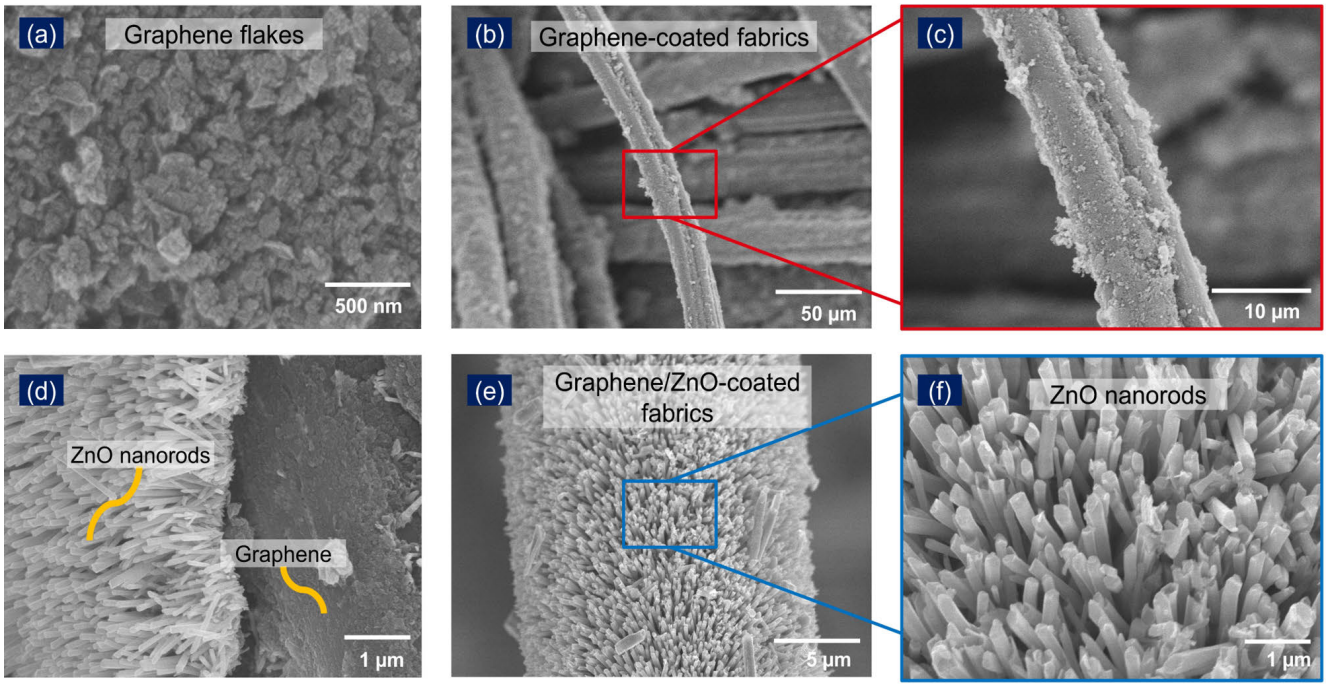

FIGURE 2. SEM images of (a) graphene flakes, (b) graphene-coated fabric, and its (c) magnified view depicting uniform material coating. (d) Boundary between ZnO nanorods and graphene. (e,f) Vertical ZnO nanorods grown on the already graphene-coated fabrics.

hydroxide and converts to ZnO upon heating, according to the following reactions:

$$(Zn(H_2O)_6)^{2+} + H_2O \leftrightarrow (Zn(H_2O)_5OH)^{+} + H_3O^{+} \quad (2)$$

$$(Zn(H_2O)_5OH)^{+} + H_2O \leftrightarrow Zn(OH)_{2(s)} + H_3O^{+} + 4H_2O \quad (3)$$

$$Zn(OH)_{2(s)} \leftrightarrow ZnO_{(s)} + H_2O \quad (4)$$

In this case, the hydrolysis equilibria of Zn^{2+} proceeds to the right to induce the simultaneous protonation of either HMTA itself or the NH_3 groups generated by the decomposition of HMTA:

$$(CH_2)_6N_4 + H_3O^{+} \leftrightarrow ((CH_2)_6N_4)H^{+} + H_2O \quad (5)$$

or

$$(CH_2)_6N_4 + 6H_2O \leftrightarrow 6HCHO + 4NH_3 \quad (6)$$

$$NH_3 + H_3O^{+} \leftrightarrow NH_4^{+} + H_2O \quad (7)$$

Therefore, the presence of the pre-deposited ZnO seed layer can promote the heterogeneous nucleation of ZnO nanorods on the fabric upon immersion and heating at 80°C. In the CBD process, HMTA is employed to induce a steric hindrance effect, in which the chelated HMTA molecules preferentially adsorb on the lateral faces of ZnO nanorods, thereby promoting the anisotropic growth of ZnO along the c-axis. Previously, the attachment of HMTA to the non-polar ZnO crystal surfaces has been proposed to occur via two possible mechanisms: through covalent bonding between the basic N donor atoms and the acidic Zn^{2+} site or through hydrogen bonding between the tertiary ammonium cations and the O^{2-} ions. Either of these can induce steric hindrance effect, which promotes the formation and growth of vertical ZnO nanorods (Fig. 2(d)-(f)). These high-aspect-ratio nanorods offer increased surfaces that will be beneficial to interact with the gas molecules. From the one of the cotton string ends, it was obvious that the ZnO nanorods were grown on that graphene (Fig. 2(d)), in which they have a diameter of ∼30 nm and heights of ∼1.5 μm. As the wet chemical method was used in this case, the employed solution could diffuse into the gaps between the strings or yarns of the dipped fabrics resulting in conformal 'wrap-around' ZnO nanorods. It is well known that the condition of the underlying layers may affect the direction and shape of the ZnO crystals during growth [49]. However, the ZnO nanostructures, which were grown on the graphene layer, employed here have similar morphology with those grown on a rigid AlN thin layer using CBD [50].

B. ELEMENTAL ANALYSIS

The elemental compositions of all samples (i.e., graphene-coated fabric, ZnO-coated fabric, and graphene/ZnO-coated fabric) were analyzed using EDS and their measurement results are shown in Fig. 3. The obtained EDS spectra have exhibited the peaks of carbon, oxygen, and zinc elements. The presence of C element in all samples indicates the carbon atoms that are originally from cellulose cotton fabrics (Table 1). This can be also observed in ZnO-coated fabric (Figure 3(b)). However, the C element in the samples of graphene-coated fabric (73.42 wt%, Fig. 3(a)) and

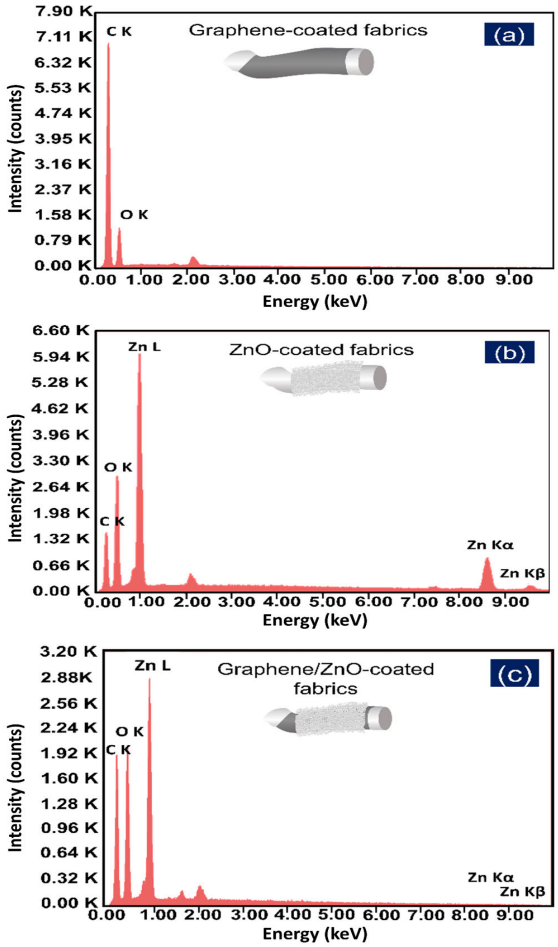

FIGURE 3. EDS spectra of three different samples, i.e., (a) graphene-coated fabric, (b) ZnO-coated fabric, and (c) graphene/ZnO-coated fabric, showing the existences of C, O, and Zn elements in all devices.

TABLE 1. Elemental concentrations of three different samples, graphene-coated fabric, Zno-coated FABRIC, graphene/Zno-coated fabric measured by EDS.

Sample	C		O		Zn	
	wt%	at%	wt%	at%	wt%	at%
Graphene-coated fabric	73.42	78.63	26.58	21.37	-	-
ZnO-coated fabric	25.52	52.02	17.38	26.60	57.10	21.38
Graphene/ZnO-coated fabric	42.11	61.54	27.65	30.34	30.24	8.12

graphene/ZnO-coated fabric (42.11 wt%, Fig. 3(c)) may also represent the presence of graphene. It was found that the graphene-coated fabric has the highest concentration of C element. Meanwhile, the strong peaks of Zn and O elements in Fig. 3(b) and (c) demonstrate the presence of ZnO nanorods on those two samples.

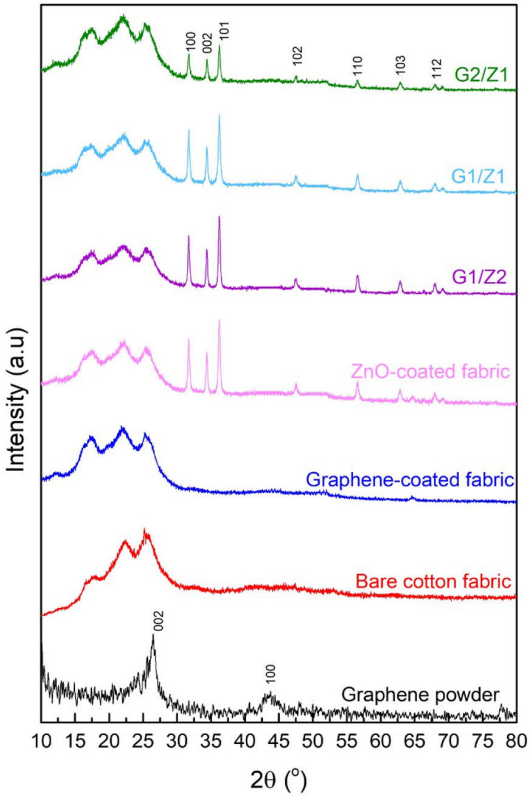

FIGURE 4. Measured XRD patterns of graphene powder, bare cotton fabric, graphene coated fabric, ZnO coated fabric, and graphene/ZnO-coated fabrics with various mixture ratios (i.e., G1/Z2, G1/Z1, and G2/Z1).

Those results suggest that the additional layer of graphene on the fabric has assisted the growth of ZnO nanorods and thus denser distribution or higher concentration of Zn can be found from the graphene/ZnO samples (Fig. 3(c)). Besides their elemental compositions, those various coated fabrics were also carefully analyzed by XRD to study their phase composition and material purity. Fig. 4 depicts the XRD spectra of different materials (i.e., graphene-coated fabric, bare cotton fabric, graphene powder, ZnO-coated fabric, G1/Z1, G2/Z1, and G1/Z2). According to the peaks of cellulose (JCPDS No. 03-0226) [59], the obtained peaks of samples containing cotton fabric are located at 2θ of 17.89°, 22.51°, and 25.51°. Meanwhile, the diffraction pattern of the graphene powder shows two distinct peaks at 2θ of 26.5° and 43°. However, in graphene/ZnO samples (i.e., G1/Z1, G2/Z1, and G1/Z2), they do not clearly show clear peaks of graphene. Instead, an overlapping of the graphene peak at 26.5° with that of cellulose at 25.51° is found. Furthermore, for the hybrid samples, the diffraction peaks at 2θ of 31.74°, 34.40°, 36.22°, 47.52°, 56.58°, 62.84° and 67.94° can be well-indexed to (100), (002), (101), (102), (110), (103) and (112) peaks of hexagonal wurtzite ZnO (JCPDS No. 36-1451), which confirm the well-produced ZnO crystal on the graphene layer. The crystallite size of the ZnO nanorods was calculated using Debye-Scherer formula [60], which is estimated to be ~25-35 nm.

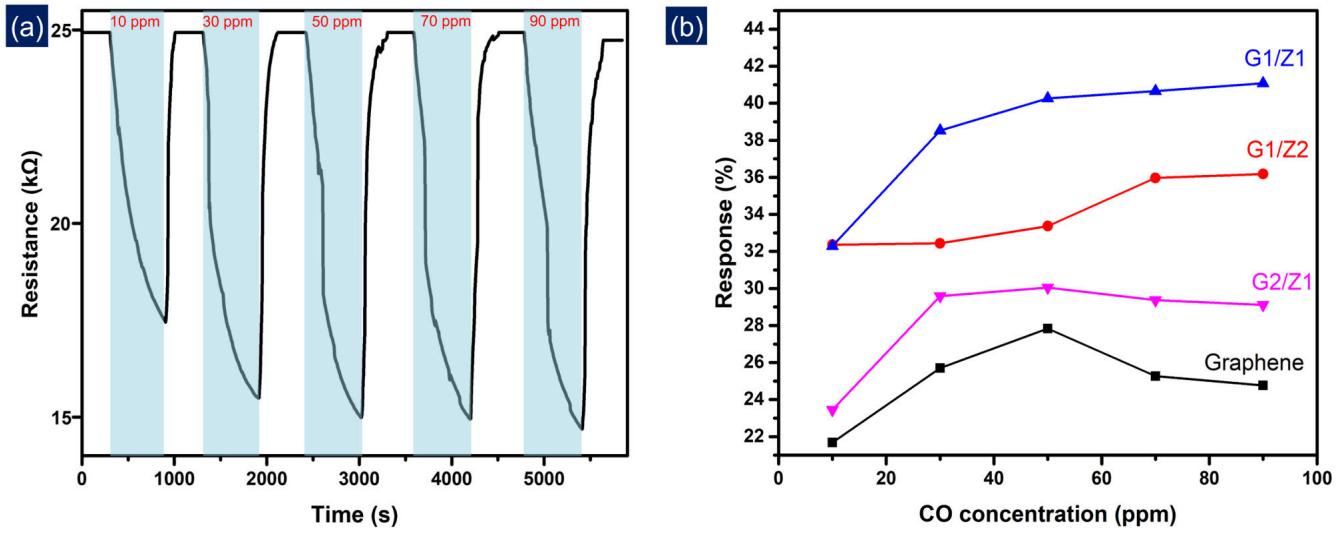

FIGURE 5. (a) Dynamic response of graphene/ZnO-coated fabric sensor (G1/Z1). (b) Response comparison of all graphene/ZnO-coated fabric sensors with different material compositions (i.e., G1/Z1, G2/Z1, G1/Z2). Graphene-coated fabric sensor was also measured to demonstrate the sensing performance enhancement of the hybrid samples. All measurements were carried out at room temperature i.e 27°C.

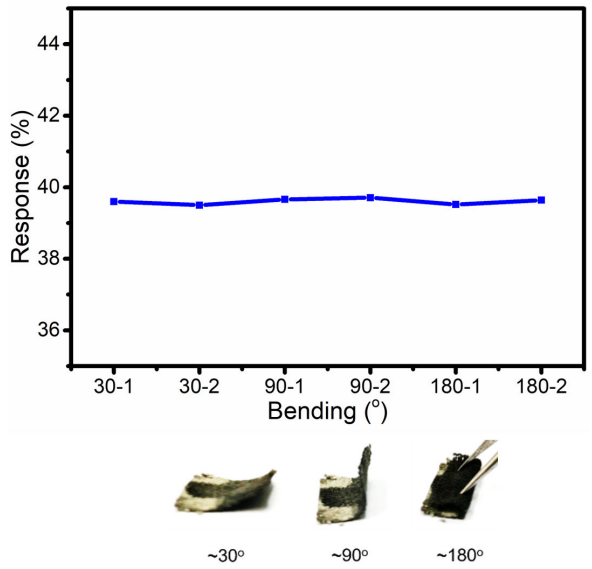

FIGURE 6. The effect of mechanical bending on the performance of G1/Z1 sensor to 50 ppm of CO at room temperature *i.e. 27° C.*

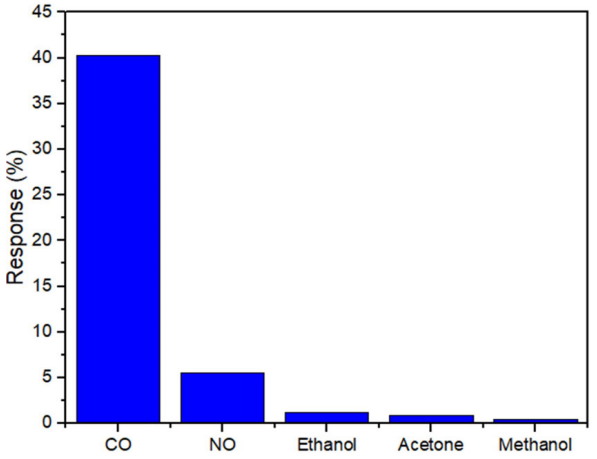

FIGURE 7. Response comparison of a graphene/ZnO-coated fabric sensor (G1/Z1) exposed to different gases (i.e., CO, NO, ethanol, acetone, and methanol) at a concentration level of 50 ppm.

C. GAS SENSOR PERFORMANCE

Fig. 5(a) displays the dynamic response-recovery behavior of the graphene/ZnO-coated fabric sensor (G1/Z1) toward different concentration levels of CO gas ranging from 10 to 90 ppm at room temperature i.e. 27 °C. Evidently, its resistance decreased as CO gas was introduced to the chamber exposing the sensitive material surfaces and subsequently increased again reaching back to the baseline or initial value after the target gas flow had been terminated. This typical behavior towards reducing gases has confirmed that the employed sensor consists of n-type semiconductor material. The response and recovery times were defined as the times to reach 90% of the final equilibrium value after the detected gas was injected and removed, respectively. The hybrid graphene/ZnO-coated fabric sensor (G1/Z1) has exhibited the response and recovery times of 435-370s and 45-115s, respectively during gas exposure assessment with CO concentrations of 10-90 ppm. As comparison, an identical sensing test procedure was applied to other hybrid samples and only graphene-coated fabric sensor, in which the measured results are shown in Fig. 5(b). Among other sensors, the hybrid graphene/ZnO-coated fabric device (G1/Z1) has obviously shown the most superior performance, while graphene-coated fabric itself exhibited the poorest response. This phenomenon has confirmed that by growing the ZnO nanorods on a graphene sheet, the gas sensor response and performance can be enhanced, in which from the experiment the ZnO:Graphene ratio is suggested to be 1:1 due

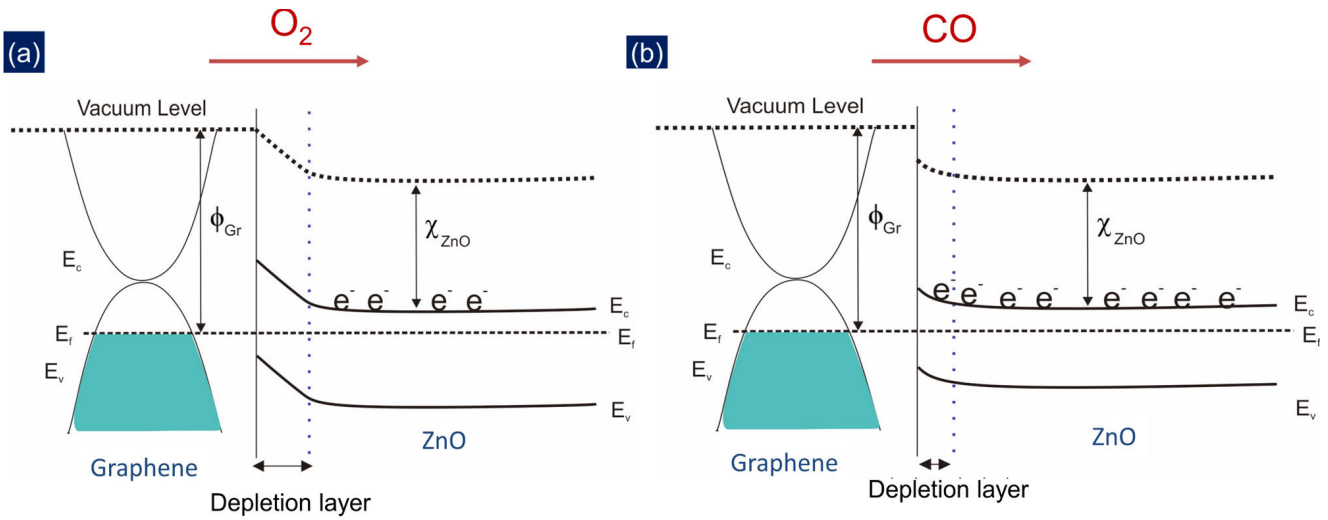

FIGURE 8. Schematic energy diagram of graphene/ZnO heterostructure (a) before and (b) after being exposed with carbon monoxide (CO) during sensor assessment.

to its strongest measured response. Besides, by increasing the ZnO amount on the hybrid sensor, the sensor response will be worsened, which might be due to the more dominant role of ZnO as the sensing material. This material has a poor response towards CO at room temperature. Normally, this device will be assisted with thermal or photoactivation methods for its operation. Moreover, in the case of hybrid graphene/ZnO-coated fabric devices of G1/Z1 and G2/Z1, they exhibit good linearity in terms of sensing response. In contrast to it, the responses of more dominant graphene sensors (i.e., G2/Z1 and only-graphene-coated sensors) were saturated and slowly started to decrease at CO concentration of ∼50 ppm. This has demonstrated that the composition of those hybrid materials should be fine adjusted, otherwise the performance of the sensor will rather degrade.

The effect of mechanical bending on the flexible sensor is an important factor for its stable performance. To check its stability, gas sensor measurements after several mechanical bending were performed. The G1/Z1 films were bendt with the angel of ∼30°, ∼90°, and ∼180° prior to the measurement. As seen in Fig. 6, the sensor delivered similar responses indicating the sensor has good stability under mechanical bending.

For completeness, we investigated the selectivity of the developed graphene/ZnO-coated fabric sensor (G1/Z1) towards some other classical gasses that are normally detected with conventional MOX sensors (e.g., NO, ethanol, acetone, and methanol). Fig. 7 depicts a comparison between responses to these gases and CO at room temperature. Concentration was kept the same for all gases to be 50 ppm. Remarkably, our sensor displayed a much higher response to CO (i.e., 40.26%) than to all those other gases (i.e., 5.48%, 1.22%, 0.9% and 0.45% for NO, ethanol, acetone, and methanol, respectively). These results have demonstrated a good selectivity of the hybrid sensor toward CO gas. Other studies stated that ZnO and graphene itself have low selectivity if they work alone [61], [47]. Our study revealed that a combination between ZnO and graphene result in synergistic effect that can improve their selectivity to CO gas. This result also comparable with other works [47], [61]. Furthermore, Table 2 has listed the outputs of previous CO sensors in the literature to be compared with those of sensor developed in this work. The proposed sensor exhibited several advantages in comparison to others because of its room operating temperature, a flexible substrate, high selectivity, and high response even in low CO concentration. Larger active surface area and activity of ZnO nanorods, as well as the synergistic effects of graphene/ZnO nanorod hybrid materials have maintained the high response to CO gas.

Humidity level is considered can strongly affect the sensor measurement. The effect of humidity on the sensor performance of G1/Z1 has been investigated. At low humidity, the response sensor value to 50 ppm of CO is 40% as the humidity level increase to medium and high, the value decreases to 36% and 27% respectively. The presence of water vapor on the sample surface can block the CO to reach the surface hence the response will be low. The more the vapor, the lower the sensor response.

D. GAS SENSING MECHANISM

Since graphene is p-type doped and ZnO is n-type semiconductor, electron transfer from ZnO to graphene occurs as their fermi levels are aligned and caused band bending as seen in Fig.8 [63]. The electron transfer occurred until the equilibrium state is reached or the fermi levels are aligned. Therefore, the potential built in was formed in the interface of graphene/ZnO. Under air atmosphere, the oxygen ion-sorption, which takes the electrons from conduction band, will enlarge the potential barrier in the junction or interface of graphene/ZnO (Fig. 8(a)). Consequently, electron transfer from CO to the system during exposure time may reduce

TABLE 2. A comparison of our proposed CO sensor with other recently developed detectors in literature.

Ref.	Materials	Sensor type	Sensing performance toward CO gas			
			CO concentration (ppm)	Operating temperature (°C)	Response (%)	Response/recovery time (s)
(38)	Graphene-ZnO on Alumina substrate	Resistive, rigid	30	300	98	-
(51)	CuO on ceramic substrate	Resistive, rigid	200	175	73	29/37
(52)	CuO on fused silica and micro-hotplate	Resistive, rigid	100-200	400	2-5	-
(53)	Al-doped ZnO on alumina substrate	Resistive, rigid	100	350	60	-
(54)	CuO-decorated graphene on PCB substrate	Resistive, rigid	0.25-1000	Room temperature	1.06-6.61	70-76/147-232
(55)	Cu-OMS-2 on insulated substrate	Resistive, rigid	10-100	Room temperature	18-33	55/42
(56)	Ag-ZnO/MoS_2 on PCB substrate	Resistive, rigid	1-1500	Room temperature	1-7	45-60/40-50
(57)	Pd-SnO_2/partially reduced graphene oxide (PRGO) on SiO_2	Resistive, rigid	50-1600	Room temperature	1-9.5	120/120
(58)	Graphene oxide on PET substrate	Voltage, flexible	50-1000	Room temperature	4.7-12	40/70
This work	**Graphene/ZnO nanorods on cotton fabrics**	**Resistive, flexible**	**10-90**	**Room temperature**	**21.68-41.08**	**435-370/45-115**

the potential and then deliver sensor responses as the change of resistance (Fig. 8(b)) [62]. Aside from the graphene role in the graphene/ZnO interface, graphene also can act as an electron channel in the composite system and cause to lower the ZnO resistance. Based on the previous studies on ZnO performance on fabric substrate [25]–[27] and our study, it was revealed that the graphene/ZnO layer in our study exhibits a lower resistance than ZnO layer. The base resistances of each sample are 3.1 KΩ, 17 KΩ, 23 KΩ, 0.26 MΩ, and >100 MΩ for graphene, G2/Z1, G1/Z1, G1/Z2, and ZnO, respectively.

The sensing mechanism of MOX semiconductor gas sensor is affected by a reaction between the gas molecule and oxygen adsorption on the MOX active surface. In the case of composite, the sensing performances are also contributed by the oxygen adsorption on the interface between the two phases. In the ambient atmosphere, oxygen molecules are adsorbed on the MOX surface and interface of graphene/ZnO, capture electrons from the conduction band and then form an oxygen ion [64]. The formation of the oxygen ions will lower the electron concentration, leading to the formation of a depletion layer. Hence, two potential barries are built on the surface of ZnO and on the interface of graphene/ZnO. The formation of the oxygen ions at room temperature is described by eqn. (8) and (9):

$$O_2(g) \rightarrow O_{2(ads)} \tag{8}$$

$$O_2(ads) + e^- \rightarrow O^-_{2(ads)} \tag{9}$$

$$O^-_{2(ads)} + 2CO = 2CO_2 + e^- \tag{10}$$

When the sensor was exposed to CO as a reducing gas, CO molecules reacted with the oxygen ions that subsequently released the electron back to the conduction band and narrowing the depletion layers. The electron release from the reaction described in Eqn (10) increases the electron concentration leading to reduction of the surface resistance of the composite [65], [66]. This phenomenon happens on the surface Regardless of successful fabrication and characterization of the hybrid graphene/ZnO nanostructures on flexible substrate for gas sensing applications, further surface analysis (e.g., X-ray photoelectron spectroscopy or Auger electron spectroscopy) and deeper analysis on the sensor mechanism are however still required for understanding the detailed surface conditions of the employed materials. Hence, the performance of the sensor can be enhanced for the next designs.

IV. CONCLUSION

Wearable CO gas sensors based on heterostructure graphene/ZnO nanorods on cotton fabrics have been realized using low-cost and low-temperature wet chemical deposition methods (i.e., dry-dipping and chemical bath deposition). Vertically aligned hexagonal ZnO nanorods have been grown

homogenously showing their good conformity over the 3D structures of the already-deposited graphene on fabrics. From electrical characterization results, the hybrid graphene/ZnO nanostructures have exhibited a lower surface resistance at room temperature compared to the surface resistance of ZnO layer due to the electron transfer from graphene to ZnO. From the gas measurement results, the presence of graphene layer underneath the ZnO has been able to improve the sensing performance of ZnO-based sensors, in which a sensing resolution down to 10 ppm can be resolved at room temperature with excellent selectivity to CO gas. To improve the performance, a basic detailed understanding of the gas sensing mechanism has to be obtained, in which more experimental analyses on the device surface conditions are required. All in all, when the mixture composition between graphene and ZnO materials can be well-controlled, these hybrid materials will have a high potential for being used as high-performance wearable gas sensors that can be integrated with, e.g., smart clothes.

REFERENCES

[1] D. Y. C. Leung, "Outdoor-indoor air pollution in urban environment: Challenges and opportunity," *Frontiers Environ. Sci.*, vol. 2, pp. 1–7, Jan. 2015.

[2] C. Chen and B. Zhao, "Review of relationship between indoor and outdoor particles: I/O ratio, infiltration factor and penetration factor," *Atmos. Environ.*, vol. 45, no. 2, pp. 275–288, Jan. 2011.

[3] O. Casals, N. Markiewicz, C. Fabrega, I. Gràcia, C. Cané, H. S. Wasisto, A. Waag, and J. D. Prades, "A parts per billion (ppb) sensor for NO_2 with microwatt (μW) power requirements based on micro light plates," *ACS Sensors*, vol. 4, no. 4, pp. 822–826, Feb. 2019.

[4] N. Markiewicz, O. Casals, C. Fabrega, I. Gràcia, C. Cané, H. S. Wasisto, A. Waag, and J. D. Prades, "Micro light plates for low-power photoactivated (gas) sensors," *Appl. Phys. Lett.*, vol. 114, no. 5, Feb. 2019, Art. no. 053508.

[5] H. S. Wasisto, E. Uhde, and E. Peiner, "Enhanced performance of pocket-sized nanoparticle exposure monitor for healthy indoor environment," *Building Environ.*, vol. 95, pp. 13–20, Jan. 2016.

[6] H. S. Wasisto, S. Merzsch, A. Stranz, A. Waag, E. Uhde, T. Salthammer, and E. Peiner, "Silicon resonant nanopillar sensors for airborne titanium dioxide engineered nanoparticle mass detection," *Sens. Actuators B, Chem.*, vol. 189, pp. 146–156, Dec. 2013.

[7] M. Bertke, J. Xu, M. Fahrbach, A. Setiono, H. Wasisto, and E. Peiner, "Strategy toward miniaturized, Self-out-Readable resonant cantilever and integrated electrostatic microchannel separator for highly sensitive airborne nanoparticle detection," *Sensors*, vol. 19, no. 4, pp. 1–12, Feb. 2019.

[8] J. Xu, M. Bertke, H. S. Wasisto, and E. Peiner, "Piezoresistive microcantilevers for humidity sensing," *J. Micromech. Microeng.*, vol. 29, no. 5, Apr. 2019, Art. no. 053003.

[9] Y. Tang, "Sources of underground CO: Crushing and ambient temperature oxidation of coal," *J. Loss Prevention Process Industries*, vol. 38, pp. 50–57, Nov. 2015.

[10] D. Penney, V. Benignus, S. Kephalopoulos, D. Kotzias, M. Kleinman, and A. Verrier, "Carbon monoxide," in *WHO Guidelines for Indoor Quality: Selected Pollutants, Geneva: World Health Organization*. Copenhagen, Denmark: World Health Organization Regional Office for Europe, 2010, p. 484.

[11] C. L. Townsend, "Effects on health of prolonged exposure to low concentrations of carbon monoxide," *Occupational Environ. Med.*, vol. 59, no. 10, pp. 708–711, Oct. 2002.

[12] B. L. Risavi, R. J. Wadas, C. Thomas, and D. F. Kupas, "A novel method for continuous environmental surveillance for carbon monoxide exposure to protect emergency medical service providers and patients," *J. Emergency Med.*, vol. 44, no. 3, pp. 637–640, Mar. 2013.

[13] F. Gullotta, A. di Masi, M. Coletta, and P. Ascenzi, "CO metabolism, sensing, and signaling," *BioFactors*, vol. 38, no. 1, pp. 1–13, Dec. 2011.

[14] G. P. Roberts, H. Youn, and R. L. Kerby, "CO-sensing mechanisms," *Microbiol. Mol. Biol. Rev.*, vol. 68, no. 3, pp. 453–473, Sep. 2004.

[15] S. Yorulmaz, "Red blood cell distribution width is an independent predictor of mortality in patients with carbon monoxide poisoning," *J. Emerg. Med. Forecast*, vol. 1, no. 1, pp. 1–4, 2018.

[16] Q. Zhou, W. Chen, L. Xu, R. Kumar, Y. Gui, Z. Zhao, C. Tang, and S. Zhu, "Highly sensitive carbon monoxide (CO) gas sensors based on ni and zn doped SnO_2 nanomaterials," *Ceram. Int.*, vol. 44, no. 4, pp. 4392–4399, Mar. 2018.

[17] E. Singh, M. Meyyappan, and H. S. Nalwa, "Flexible graphene-based wearable gas and chemical sensors," *ACS Appl. Mater. Inter.*, vol. 9, no. 40, pp. 34544–34586, Sep. 2017.

[18] N. Tang, C. Zhou, L. Xu, Y. Jiang, H. Qu, and X. Duan, "A fully integrated wireless flexible ammonia sensor fabricated by soft nano-lithography," *ACS Sensors*, vol. 4, no. 3, pp. 726–732, Feb. 2019.

[19] M. G. Chung, D.-H. Kim, D. K. Seo, T. Kim, H. U. Im, H. M. Lee, J.-B. Yoo, S.-H. Hong, T. J. Kang, and Y. H. Kim, "Flexible hydrogen sensors using graphene with palladium nanoparticle decoration," *Sens. Actuators B, Chem.*, vol. 169, pp. 387–392, Jul. 2012.

[20] H.-D. Zhang, C.-C. Tang, Y.-Z. Long, J.-C. Zhang, R. Huang, J.-J. Li, and C.-Z. Gu, "High-sensitivity gas sensors based on arranged polyaniline/PMMA composite fibers," *Sens. Actuators A, Phys.*, vol. 219, pp. 123–127, Nov. 2014.

[21] X. Wang, J. Li, H. Song, H. Huang, and J. Gou, "Highly stretchable and wearable strain sensor based on printable carbon nanotube Layers/Polydimethylsiloxane composites with adjustable sensitivity," *ACS Appl. Mater. Inter.*, vol. 10, no. 8, pp. 7371–7380, Feb. 2018.

[22] S.-J. Young and Z.-D. Lin, "Ethanol gas sensors composed of carbon nanotubes with au nanoparticles adsorbed onto a flexible PI substrate," *ECS J. Solid State Sci. Technol.*, vol. 6, no. 10, pp. M130–M132, Nov. 2017.

[23] C. Bali, A. Brandlmaier, A. Ganster, O. Raab, J. Zapf, and A. Hübler, "Fully inkjet-printed flexible temperature sensors based on carbon and PEDOT:PSS1," *Mater. Today, Proc.*, vol. 3, no. 3, pp. 739–745, 2016.

[24] S. Li, "The room temperature gas sensor based on Polyaniline flower-like WO3 nanocomposites and flexible PET substrate for NH_3 detection," *Sens. Actuators B, Chem.*, vol. 259, pp. 505–513, 2017.

[25] Z. H. Lim, Z. X. Chia, M. Kevin, A. S. W. Wong, and G. W. Ho, "A facile approach towards ZnO nanorods conductive textile for room temperature multifunctional sensors," *Sens. Actuators B, Chem.*, vol. 151, no. 1, pp. 121–126, Nov. 2010.

[26] J. Cao and C. Wang, "Multifunctional surface modification of silk fabric via graphene oxide repeatedly coating and chemical reduction method," *Appl. Surf. Sci.*, vol. 405, pp. 380–388, May 2017.

[27] S. M. Mohammad, Z. Hassan, R. A. Talib, N. M. Ahmed, M. A. Al-Azawi, N. M. Abd-Alghafour, C. W. Chin, and N. H. Al-Hardan, "Fabrication of a highly flexible low-cost H_2 gas sensor using ZnO nanorods grown on an ultra-thin nylon substrate," *J. Mater. Sci., Mater. Electron.*, vol. 27, no. 9, pp. 9461–9469, May 2016.

[28] T. J. Athauda, U. S. K. Madduma-Bandarage, and Y. Vasquez, "Integration of ZnO/ZnS nanostructured materials into a cotton fabric platform," *RSC Adv.*, vol. 4, no. 106, pp. 61327–61332, 2014.

[29] V. Pandiyarasan, J. Archana, A. Pavithra, V. Ashwin, M. Navaneethan, Y. Hayakawa, and H. Ikeda, "Hydrothermal growth of reduced graphene oxide on cotton fabric for enhanced ultraviolet protection applications," *Mater. Lett.*, vol. 188, pp. 123–126, Feb. 2017.

[30] H. Park, F. Tong, A. Sujan, Y. Chung, M. Park, B. J. Tatarchuk, H. Koo, H. Ahn, Y. S. Yoon, and D.-J. Kim, "Growth of nanostructured ZnO on wearable fabrics for functional garment," *Mater. Lett.*, vol. 118, pp. 47–50, Mar. 2014.

[31] B. Xu and Z. Cai, "Fabrication of a superhydrophobic ZnO nanorod array film on cotton fabrics via a wet chemical route and hydrophobic modification," *Appl. Surf. Sci.*, vol. 254, no. 18, pp. 5899–5904, Jul. 2008.

[32] T. J. Athauda, W. S. LePage, J. M. Chalker, and R. R. Ozer, "High density growth of ZnO nanorods on cotton fabric enables access to a flame resistant composite," *RSC Adv.*, vol. 4, no. 28, pp. 14582–14585, 2014.

[33] Q. Xu, L. Xie, H. Diao, F. Li, Y. Zhang, F. Fu, and X. Liu, "Antibacterial cotton fabric with enhanced durability prepared using silver nanoparticles and carboxymethyl chitosan," *Carbohydrate Polym.*, vol. 177, pp. 187–193, Dec. 2017.

[34] M.-A. Kang, S. Ji, S. Kim, C.-Y. Park, S. Myung, W. Song, S. S. Lee, J. Lim, and K.-S. An, "Highly sensitive and wearable gas sensors consisting of chemically functionalized graphene oxide assembled on cotton yarn," *RSC Adv.*, vol. 8, no. 22, pp. 11991–11996, 2018.

[35] Y. Ju Yun, W. G. Hong, N.-J. Choi, B. Hoon Kim, Y. Jun, and H.-K. Lee, "Ultrasensitive and highly selective graphene-based single yarn for use in wearable gas sensor," *Sci. Rep.*, vol. 5, no. 1, pp. 1–7, Jun. 2015.

[36] Y. J. Yun, W. G. Hong, D. Y. Kim, H. J. Kim, Y. Jun, and H.-K. Lee, "E-textile gas sensors composed of molybdenum disulfide and reduced graphene oxide for high response and reliability," *Sens. Actuators B, Chem.*, vol. 248, pp. 829–835, Sep. 2017.
[37] D. K. Subbiah, G. K. Mani, K. J. Babu, A. Das, and J. B. B. Rayappan, "Nanostructured ZnO on cotton fabrics—A novel flexible gas sensor & UV filter," *J. Clean. Prod.*, vol. 194, pp. 372–382, 2018.
[38] A. R. Muchtar, N. L. W. Septiani, M. Iqbal, A. Nuruddin, and B. Yuliarto, "Preparation of graphene–zinc oxide nanostructure composite for carbon monoxide gas sensing," *J. Electron. Mater.*, vol. 47, pp. 3647–3656, 2018.
[39] S. S. Low, M. T. T. Tan, H.-S. Loh, P. S. Khiew, and W. S. Chiu, "Facile hydrothermal growth graphene/ZnO nanocomposite for development of enhanced biosensor," *Analytica Chim. Acta*, vol. 903, pp. 131–141, Jan. 2016.
[40] K. Anand, O. Singh, M. P. Singh, J. Kaur, and R. C. Singh, "Hydrogen sensor based on graphene/ZnO nanocomposite," *Sens. Actuators B, Chem.*, vol. 195, no. 2, pp. 409–415, May 2014.
[41] Y. Zhao, L. Liu, T. Cui, G. Tong, and W. Wu, "Enhanced photocatalytic properties of ZnO/reduced graphene oxide sheets (rGO) composites with controllable morphology and composition," *Appl. Surf. Sci.*, vol. 412, pp. 58–68, Aug. 2017.
[42] W. Yuan and G. Shi, "Graphene-based gas sensors," *J. Mater. Chem. A*, vol. 1, no. 35, pp. 10078–10091, 2013.
[43] A. R. Marlinda, N. M. Huang, M. R. Muhamad, M. N. An'Amt, B. Y. S. Chang, N. Yusoff, I. Harrison, H. N. Lim, C. H. Chia, and S. V. Kumar, "Highly efficient preparation of ZnO nanorods decorated reduced graphene oxide nanocomposites," *Mater. Lett.*, vol. 80, pp. 9–12, Aug. 2012.
[44] B. Saravanakumar, R. Mohan, and S.-J. Kim, "Facile synthesis of graphene/ZnO nanocomposites by low temperature hydrothermal method," *Mater. Res. Bull.*, vol. 48, no. 2, pp. 878–883, Feb. 2013.
[45] Z. Liu, L. Yu, F. Guo, S. Liu, L. Qi, M. Shan, and X. Fan, "Facial development of high performance room temperature NO_2 gas sensors based on ZnO nanowalls decorated rGO nanosheets," *Appl. Surf. Sci.*, vol. 423, pp. 721–727, Nov. 2017.
[46] X. Li, J. Wang, D. Xie, J. Xu, R. Dai, L. Xiang, H. Zhu, and Y. Jiang, "Reduced graphene oxide/hierarchical flower-like zinc oxide hybrid films for room temperature formaldehyde detection," *Sens. Actuators B, Chem.*, vol. 221, pp. 1290–1298, Dec. 2015.
[47] G. Singh, A. Choudhary, D. Haranath, A. G. Joshi, N. Singh, S. Singh, and R. Pasricha, "ZnO decorated luminescent graphene as a potential gas sensor at room temperature," *Carbon*, vol. 50, no. 2, pp. 385–394, Feb. 2012.
[48] H. Tai, Z. Yuan, W. Zheng, Z. Ye, C. Liu, and X. Du, "ZnO Nanoparticles/Reduced graphene oxide bilayer thin films for improved NH_3-sensing performances at room temperature," *Nanosc. Res. Lett.*, vol. 11, no. 1, Mar. 2016.
[49] S.-H. Park, S.-Y. Seo, S.-H. Kim, and S.-W. Han, "Surface roughness and strain effects on ZnO nanorod growth," *Appl. Phys. Lett.*, vol. 88, no. 25, Jun. 2006, Art. no. 251903.
[50] T. Granz, "UV-LED photo-activated room temperature no. 2, sensors based on nanostructured ZnO/AlN thin films," in *Proc. Multidisciplinary Digit. Publishing Inst. Proc.*, 2019, vol. 2, no. 13, p. 888.
[51] L. Hou, C. Zhang, L. Li, C. Du, X. Li, X.-F. Kang, and W. Chen, "CO gas sensors based on p-type CuO nanotubes and CuO nanocubes: Morphology and surface structure effects on the sensing performance," *Talanta*, vol. 188, pp. 41–49, Oct. 2018.
[52] L. Presmanes, Y. Thimont, I. El Younsi, A. Chapelle, F. Blanc, C. Talhi, C. Bonningue, A. Barnabé, P. Menini, and P. Tailhades, "Integration of P-CuO thin sputtered layers onto microsensor platforms for gas sensing," *Sensors*, vol. 17, no. 6, pp. 1–17, Jun. 2017.
[53] S. K. Lim, S. H. Hong, S.-H. Hwang, W. M. Choi, S. Kim, H. Park, and M. G. Jeong, "Synthesis of al-doped ZnO nanorods via microemulsion method and their application as a CO gas sensor," *J. Mater. Sci. Technol.*, vol. 31, no. 6, pp. 639–644, Jun. 2015.
[54] D. Zhang, C. Jiang, J. Liu, and Y. Cao, "Carbon monoxide gas sensing at room temperature using copper oxide-decorated graphene hybrid nanocomposite prepared by layer-by-layer self-assembly," *Sens. Actuators B, Chem.*, vol. 247, pp. 875–882, Aug. 2017.
[55] R. Kumar, J. Mittal, N. Kushwaha, B. V. Rao, S. Pandey, and C.-P. Liu, "Room temperature carbon monoxide gas sensor using cu doped OMS-2 nanofibers," *Sens. Actuators B, Chem.*, vol. 266, pp. 751–760, Aug. 2018.
[56] D. Zhang, Y. Sun, C. Jiang, Y. Yao, D. Wang, and Y. Zhang, "Room-temperature highly sensitive CO gas sensor based on ag-loaded zinc oxide/molybdenum disulfide ternary nanocomposite and its sensing properties," *Sens. Actuators B, Chem.*, vol. 253, pp. 1120–1128, Dec. 2017.
[57] M. Shojaee, S. Nasresfahani, and M. H. Sheikhi, "Hydrothermally synthesized pd-loaded SnO_2/partially reduced graphene oxide nanocomposite for effective detection of carbon monoxide at room temperature," *Sens. Actuators B, Chem.*, vol. 254, pp. 457–467, Jan. 2018.
[58] S. Sayed and A. A. El-moneim, "High performance carbon monoxide gas sensor based on graphene," *Int. J. Eng. Res. Technol.*, vol. 4, no. 6, pp. 518–523, 2015.
[59] T. J. Athauda, P. Hari, and R. R. Ozer, "Tuning physical and optical properties of ZnO nanowire arrays grown on cotton fibers," *ACS Appl. Mater. Inter.*, vol. 5, no. 13, pp. 6237–6246, Jun. 2013.
[60] V. Khranovskyy, "Structural and morphological properties of ZnO:Ga thin films," *Thin Solid Films*, vol. 515, no. 2, pp. 472–476, 2006.
[61] N. H. Ha, D. D. Thinh, N. T. Huong, N. H. Phuong, P. D. Thach, and H. S. Hong, "Fast response of carbon monoxide gas sensors using a highly porous network of ZnO nanoparticles decorated on 3D reduced graphene oxide," *Appl. Surf. Sci.*, vol. 434, pp. 1048–1054, Mar. 2018.
[62] N. L. W. Septiani, Y. V. Kaneti, B. Yuliarto, H. K. Dipojono, T. Takei, J. You, and Y. Yamauchi, "Hybrid nanoarchitecturing of hierarchical zinc oxide wool-ball-like nanostructures with multi-walled carbon nanotubes for achieving sensitive and selective detection of sulfur dioxide," *Sens. Actuators B, Chem.*, vol. 261, pp. 241–251, May 2018.
[63] R. Liu, X.-C. You, X.-W. Fu, F. Lin, J. Meng, D.-P. Yu, and Z.-M. Liao, "Gate modulation of graphene-ZnO nanowire Schottky diode," *Sci. Rep.*, vol. 5, no. 1, p. 10125, May 2015.
[64] D. Zhang, Z. Wu, and X. Zong, "Metal-organic frameworks-derived zinc oxide nanopolyhedra/S, N: Graphene quantum dots/polyaniline ternary nanohybrid for high-performance acetone sensing," *Sens. Actuators B, Chem.*, vol. 288, pp. 232–242, Jun. 2019.
[65] Z. Yang, D. Zhang, and D. Wang, "Carbon monoxide gas sensing properties of metal-organic frameworks-derived, sctin dioxide nanoparticles/molybdenum diselenide nanoflowers," *Sens. Actuators B*, vol. 304, 2020, Art. no. 127369.
[66] D. Zhang, J. Wu, and Y. Cao, "Cobalt-doped indium oxide/molybdenum disulfide ternary nanocomposite toward carbon monoxide gas sensing," *J. Alloys Compounds*, vol. 777, pp. 443–453, Mar. 2019.

LISTYA UTARI received the B.Sc. degree in physics from the Indonesia University of Education, Bandung, in 2015, and the M.Sc. degree in physics engineering from the Institut Teknologi Bandung, in 2018. Her research interests mainly in nanomaterials, especially ZnO, and for flexible gas sensor.

NI LUH WULAN SEPTIANI received the B.Sc. degree in physics from the Indonesia University of Education, Bandung, Indonesia, and the M.Sc. degree in engineering physics from the Institut Teknologi Bandung, Bandung, where she is currently pursuing the Ph.D. program in engineering physics. Her research interest includes the development of nanocomposite material for energy and environmental application.

SUYATMAN received the B.S. degree from the Engineering Physics Department, Institut Teknologi Bandung, Bandung, Indonesia, the master's degrees from Tohoku University, Tohoku, Japan, and the Ph.D. degree from INP Grenoble, Grenoble, French, in 1997. He is currently an Associate Professor with the Department of Engineering Physics, Faculty of Industrial Technology, Institut Teknologi Bandung. His research interests are magnetite nanomaterials for medical application, and nanomaterial for environmetal and energy application.

NUGRAHA received the B.S. degree from the Engineering Physics Department, Institut Teknologi Bandung, Bandung, Indonesia, and the master's and Ph.D. degrees from Tohoku University, Tohoku, Japan. He is currently an Associate Professor with the Department of Engineering Physics, Faculty of Industrial Technology, Institut Teknologi Bandung. His research interests are crystal growth and nanomaterials for energy and environment application.

LEVY OLIVIA NUR received the B.S., master's, and Ph.D. degrees from the electrical engineering Department, Institut Teknologi Bandung, Bandung, Indonesia. She is currently an Associate Professor with the Department of Telecommunication Engineering, Faculty of Electrical and Communication Engineering, Telkom University, Bandung. Her research interests are microwave absorbent material, metamaterial, and electromagnetic wave propagation.

HUTOMO SURYO WASISTO received the Dr.Ing. degree (Hons.) in electrical engineering from Technische Universität (TU) Braunschweig, Braunschweig, Germany, in 2014. Since 2016, he has been the Head of the LENA-OptoSense Group, TU Braunschweig. His current research interests include nano-scaled sensors, optoelectronics, and electronics.

BRIAN YULIARTO received the B.S. degree from the Engineering Physics Department, Institut Teknologi Bandung, Bandung, Indonesia, and the M.Eng. and Ph.D. degrees from the Department of Quantum Engineering and Systems Science, The University of Tokyo, Tokyo, Japan. He is currently a Full Professor with the Department of Engineering Physics, Faculty of Industrial Technology, Institut Teknologi Bandung, where he is also the Head of the Department of Engineering Physics. His research interests are nanomaterials development for energy and environmental application, and have published more than 50 articles in his research area.